

# Assessing Adequate Voltage Stability Analysis Tools for Networks with High Wind Power Penetration

Federico Milano, *Member, IEEE*

**Abstract**— This paper presents a comparison of static and dynamic continuation power flow techniques, time domain simulations and quasi-static time domain simulations for voltage stability analysis of networks with high wind power penetration. Three wind turbine models are considered, namely, constant-speed induction generator; doubly-fed induction generator; and direct-drive synchronous generator. Several simulations are solved in order to assess the behavior of wind turbine models and the reliability of voltage stability techniques. The case study is based on a 40-bus network that models an existing distribution system with one high voltage feeder.

**Index Terms**— Voltage stability, embedded wind generation, continuation power flow, reactive power adequacy, distribution network.

## I. INTRODUCTION

In recent years, due to environmental constraints and political incentives, wind power penetration has been constantly increasing in most developed countries all around the world [1]–[3]. Since the level of wind power is becoming a relevant percentage of the total installed power (e.g. about 15% in Spain), it is necessary to worry about stability issues that can be originated by wind generation.

This paper considers static and dynamic models of embedded wind generators (EWGs) for voltage stability analysis. In particular, static wind plants are modeled as constant PQ generators, as the wind parks are typically regulated with constant power factor. In order to observe the effect of voltage regulation of wind plants, also a constant PV model with realistic reactive power limits is considered. Dynamic models used in this paper are: constant speed induction generator (CSIG), variable speed doubly-fed induction generators (DFIG), and variable speed direct drive synchronous generators (DDSG). Accurate wind speed, turbine and regulator models are also taken into account. Regulators are: pitch control (for variable speed turbines) [4], voltage control [5], [6], and wind turbine power control [7].

Although voltage control is possible, EWGs are typically operated with constant power factor close to one. If the wind power penetration is large with respect to the total power generation, transient stability [8], fault analysis [9] and short term voltage stability [10] are relevant phenomena. Due to the actual trend of increasing wind power penetration in developed countries all around the world, long term voltage stability is more and more an actual issue. Reference [11] focuses on long

term voltage stability analysis based on the continuation power flow technique, while [12], [13] [14] and [15] discuss wind power penetration in distribution networks. Finally, reference [16] focuses on maximizing the wind penetration in existing distribution networks.

This paper presents a comparison of static and dynamic continuation power flow techniques (SCPF and DCPF) [17], time domain simulations (TDS) and quasi-static time domain simulations (QSTDS) for voltage stability analysis of networks with high wind power penetration.

The case studies that are presented in the paper are based on a 40-bus network that models a realistic “weak” distribution system with one high voltage feeder. Several simulations are solved in order to assess the features and reliability of static and dynamic EWG models and voltage stability techniques. For each EWG model (namely, CSIG, DFIG and DDSG) five simulations are considered, as follows:

- 1) SCPF with constant PQ model.
- 2) SCPF with constant PV model and reactive power limits.
- 3) DCPF with voltage control, wind power control and, if applicable, pitch control limits.
- 4) QSTDS with a “slow” wind ramp that simulates a power output increase of wind generators.
- 5) TDS with a 15-second wind ramp that simulates a fast power output increase of wind generators.

This paper is organized as follows. Section II provides a brief mathematical formulation of the proposed voltage stability assessment tools. Section III describes the models pertaining to the wind turbines and induction and synchronous generators. Section IV is a case study based on a 40-bus model of the Southwest England distribution network [18]. Section V gives relevant conclusions.

## II. VOLTAGE STABILITY ASSESSMENT TOOLS

### A. System Model

The power system is modeled as a set of nonlinear differential algebraic equations DAE:

$$\begin{aligned} \dot{x} &= f(x, y, u, \lambda) \\ 0 &= g(x, y, u, \lambda) \end{aligned} \quad (1)$$

where  $y$  ( $y \in \mathbb{R}^m$ ) are the algebraic variables, i.e. voltage amplitudes  $V$  and phases  $\theta$  at the network buses and all other algebraic variables such as generator field voltages, AVR reference voltages, etc.,  $x$  ( $x \in \mathbb{R}^n$ ) are the state variables,  $u$  ( $u \in \mathbb{R}^p$ ) are controllable input variables, such as reference voltages of AVRs, and  $\lambda$  ( $\lambda \in \mathbb{R}^\ell$ ) are non-controllable variables such as the wind speed. In this paper  $\ell = 1$ , thus  $\lambda$  is a scalar quantity that measures the generation margin of

F. Milano is with University of Castilla-La Mancha, Spain, e-mail Federico.Milano@uclm.es.

F. Milano is partly supported by the Ministry of Science and Technology of Spain through CICYT Project DPI2006-08001; and by the Junta de Comunidades de Castilla-La Mancha, through projects PBI-05-053 and PCI-08-0102.

EWGs. Equations  $g$  ( $g \in \mathbb{R}^m$ ) are the algebraic equations that include power flow equations, and  $f$  ( $f \in \mathbb{R}^n$ ) are the differential equations.

### B. Static Continuation Power Flow

The static continuation power flow (SCPF) technique takes into account standard power flow models, i.e. constant PV or PQ generators with reactive power limits, and static PQ or voltage dependent loads. The interested reader can find a detailed description of the standard continuation power flow analysis in [17]. The stability information that can be obtained by the SCPF is typically associated to the maximum loading margin of the system. However, since this paper focuses on wind penetration, the stability margin  $\lambda$  is defined in this paper as a measure of the maximum level of wind power generation. This margin is limited by voltage stability limits (saddle-node bifurcation or limit-induced bifurcation) or security limits (voltage limits, transmission line thermal limits).

For the SPCF, (1) becomes:

$$0 = g(y, u, \lambda) \quad (2)$$

Wind generators are modeled as standard PQ or PV generators with reactive power limits and the generation margin  $\lambda$  multiplies all active generator power. The slack bus, which is assumed to be the high voltage feeder, is not multiplied by  $\lambda$  and can reverse its flow for high wind power penetration.

### C. Dynamic Continuation Power Flow

The dynamic continuation power flow (DCPF) technique considers dynamic models of generators, loads and controllers and computes the equilibrium points as the wind power generation level increases. The DCPF also allows obtaining information about the maximum loading level of the system. The bounds that can be taken into account by the DCPF are the same as SCPF plus dynamic bifurcations, such as Hopf bifurcations. Furthermore, since regulators (e.g. AVR and turbine governors) are modeled with detailed differential algebraic equations, the DCPF analysis is more precise than SCPF for determining the loading level of a system.

For the SPCF, (1) becomes:

$$\begin{aligned} 0 &= f(x, y, u, \lambda) \\ 0 &= g(x, y, u, \lambda) \end{aligned} \quad (3)$$

Wind generators are modeled with their full DAE equations. In this case the generation margin  $\lambda$  multiplies all wind speeds that feed wind turbines. The slack bus, which is assumed to be the high voltage feeder, is modeled as an infinite inertia generator.

### D. Quasi-static Time Domain Simulation

Quasi-static time domain simulation (QSTDS) is similar to the DCPF, but in this case the wind power generation level increases “slowly” as a function of time. The main difference of the QSTDS with respect to the DCPF is that the effects of the wind generation ramp are more realistically modeled.

For the QSTDS, (1) becomes:

$$\begin{aligned} 0 &\approx \dot{x} = f(x, y, u, \lambda(t)) \\ 0 &= g(x, y, u, \lambda(t)) \end{aligned} \quad (4)$$

### E. Time Domain Simulation

Finally, standard time domain simulations (TDS) present non-negligible time derivatives during the transients. TDS are useful to assess the time response of controllers to fast power variations of wind turbines. In this case, the wind speed is assumed to undergo a fast ramp, thus system dynamics cannot be neglected. The system is described by (1).

## III. MODELING OF WIND TURBINES AND GENERATORS

Three models of wind turbines are considered in this paper: constant speed induction generator wind turbine with squirrel cage induction generator (CSIG), variable speed wind turbine with doubly-fed (wound rotor) induction generator (DFIG) and variable speed wind turbine with direct-drive synchronous generator (DDSG). Controls and converter models are included in the wind turbine equations. Wind turbine models presented here are mostly based on models discussed in [8]. Figure 1 depicts the three wind turbines types. Due to space limitations, following subsections only provide brief outlines of the EWG models. Full mathematical models can be found in [19].

### A. Constant Speed Induction Generator

The simplified electrical circuit used for the squirrel cage induction generator is the same as the one for the single-cage induction motor, the only difference with respect to the induction motor being that the currents are positive if injected in the network. A fixed capacitor bank is added at the EWG busbar to provide the reactive power needed by the induction generator and to maintain a power factor equal to one at the network point of connection. The mechanical differential equations take into account the turbine and rotor inertias and shaft stiffness [20]. The *tower shadow* effect is taken into account through a small-magnitude (0.025 p.u.) periodic torque pulsation as described in [21].

### B. Doubly-fed Induction Generator

Steady-state electrical equations of the doubly fed induction generator are assumed, as the stator and rotor flux dynamics are fast in comparison with grid dynamics and the converter controls basically decouple the generator from the grid.

The generator active and reactive powers depend on the stator and converter currents. Due to the converter operation mode, the power injected in the grid can be written as a function of stator and rotor currents. Assuming a lossless converter model, the active power of the converter coincides with the rotor active power. The reactive power injected into the grid can be approximated neglecting stator resistance and assuming that the  $d$ -axis coincides with the maximum of the stator flux.

The generator motion equation is modeled as a single shaft, as it is assumed that the converter controls are able to filter

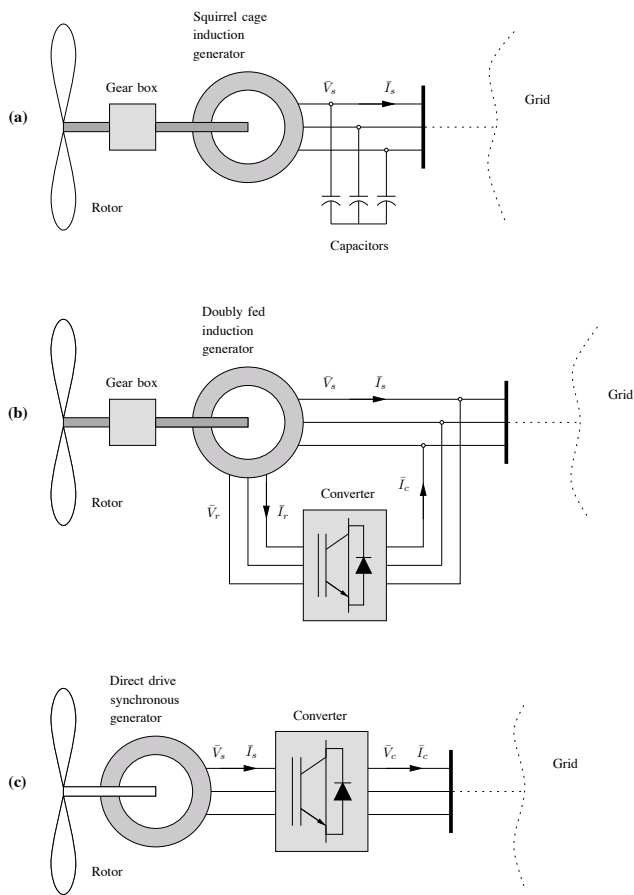


Fig. 1. Wind turbine types. (a) Constant speed wind turbine with squirrel cage induction generator; (b) Variable speed wind turbine with doubly fed induction generator; (c) Variable speed wind turbine with direct drive synchronous generator.

shaft dynamics. For the same reason, no tower shadow effect is considered in this model.

Converter dynamics are highly simplified, as they are fast with respect to the electromechanical transients. Thus, the converter is modeled as an ideal current source, where the rotor direct and quadrature currents are state variables and are used for the rotor speed control and the voltage control, respectively. It is assumed that the wind power  $P_w = 0$  if  $\omega_m < 0.5$  p.u. and that  $P_w = 1$  p.u. if the rotor mechanical speed  $\omega_m > 1$  p.u. Thus, the rotor speed control only has effect for sub-synchronous speeds [7]. Both the speed and voltage controls undergo anti-windup limiters in order to avoid converter over-currents [5], [6]. Finally, the pitch control works only for super-synchronous speeds. An anti-windup limiter locks the pitch angle to  $\theta_p = 0$  for sub-synchronous speeds [4].

### C. Direct-drive Synchronous Generator

Steady-state electrical equations of the direct drive synchronous generator are assumed, as the stator and rotor flux dynamics are fast in comparison with grid dynamics and the converter controls basically decouple the generator from the grid. We assume a lossless converter and a power factor equal

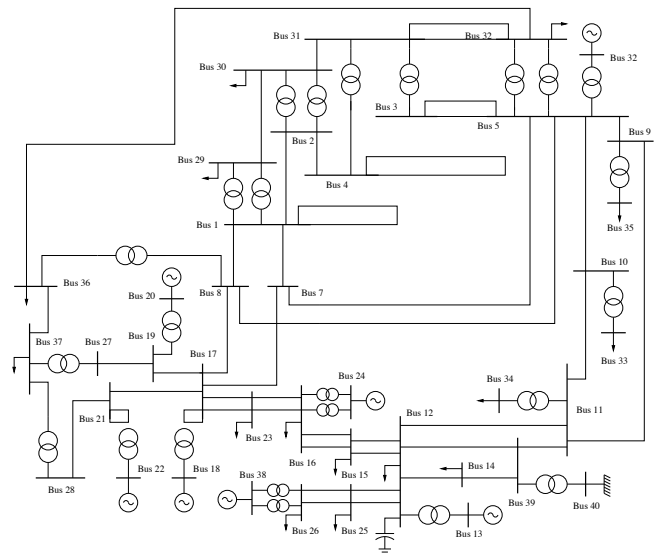


Fig. 2. 40-bus test system.

to 1. Furthermore, the reactive power injected into the grid is controlled by means of the converter direct current.

The generator motion equation is modeled as a single shaft, as it is assumed that the converter controls are able to filter shaft dynamics. As a consequence, no tower shadow effect is considered in this model. The mechanical torque and power are modeled as in the doubly fed induction motor.

The converter is highly simplified and is modeled as an ideal current source, where generator stator direct and quadrature currents, and the converter direct current are state variables and are used for the rotor speed control and the reactive power control and the voltage control, respectively.

The power-speed characteristic is computed in a similar way as for DFIG models. Rotor speed, pitch and voltage controls are the same as those used for the DFIG model.

## IV. CASE STUDIES

This section describes a variety of case studies based on a 40-bus test system. All static and dynamic simulations were solved using the software package PSAT [22].

Figure 2 depicts a partly meshed 40-bus distribution network. This system is partly based on a simplified model of the Southwest England power system. Most power flow data of the test system can be found in [18] while other data that refer to EWGs and control schemes are provided in [15]. The network presents 40 buses, 65 lines and 17 loads for a total load of about 41 MW and 7 MVar. There are three voltage levels, namely 132, 33 and 11 kV. The feeding substation is located at bus 40 at 132 kV. Buses 20, 22, and 29-37 are at 11 kV, while all remaining buses are at 33 kV. EWGs are located at buses 6, 13, 18, 20, 22, 24 and 38. Furthermore all EWGs have a nominal power of 20 MVA. Reactive power limits of EWGs are taken into account in all simulations. EWG active power limits are neglected in the static and dynamic CPF analyses, as it is common practice. However, active power limits are considered in the dynamic simulations for DFIGs and DDSGs through the power and pitch angle controls.

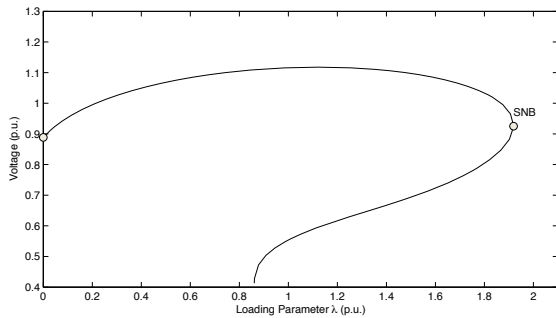


Fig. 3. Voltage at bus 29 as a function of the generation margin  $\lambda$ . EWGs are modeled as constant PQ generators.  $\lambda_{\max} = 1.9185$

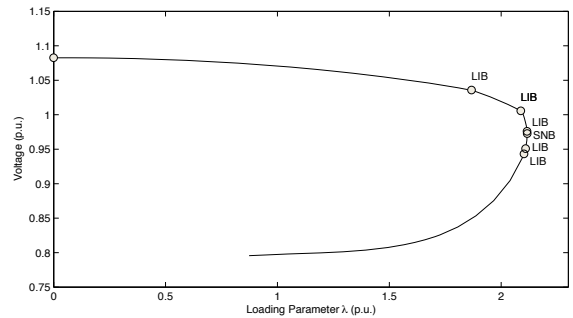


Fig. 4. Voltage at bus 29 as a function of the generation margin  $\lambda$ . EWGs are modeled as constant PV generators.  $\lambda_{\max} = 2.1162$

Figure 3 shows the nose curve of a representative voltage of the system as a function of the generation margin  $\lambda$ . The EWGs only generate active powers and are modeled as constant PQ generators. CSIG cannot control the reactive power, as their capacitor banks are fixed; however, the approximation of considering constant reactive power ( $q_G = 0$ ) for CSIG is acceptable and does not affect results. For  $\lambda = 0$ , there is no wind generation, while  $\lambda = 0$  corresponds to a medium level EWGs generation. In the first half of the curve the voltage increases. This behavior is due to the fact that the HV feeder is decreasing its power injection into the distribution network. In the second half of the curve, the voltage decreases, as it is usual in nose curves. This happens because the feeder reverts its power flow and the EWGs are not only supplying local loads but also supplying power to the HV network. Since active power limits are not enforced and transmission line limits are considered to be high, the system collapses at a saddle-node bifurcation for  $\lambda_{\max} = 1.9185$ .

Figure 4 shows the nose curve of a representative voltage of the system as a function of the generation margin  $\lambda$ . We assume that EWGs generates active powers and control the voltage (constant PV model). CSIG cannot control the voltage, thus the PV model is adequate only for DFIGs and DDSGs. The voltage regulations allow increasing the generator margin ( $\lambda_{\max} = 2.1162$ ) with respect to the constant PQ generator model. Observe that several limit-induced bifurcations occurs before the voltage collapse. It is worth to be noted that the voltage is always higher than 1 p.u., even close to the SNB. Thus the voltage collapse cannot be forecasted based only on voltage measures.

Figure 5 shows the wind speed ramps used for the quasi-static time domain simulations (QSTDS). The wind speed ramps simulate the increase of the wind power generation and their effect is thus similar to the generation margin  $\lambda$ . Wind speeds close to 1 p.u. corresponds to a medium-level wind power generation. In the following, EWGs are modeled with their detailed DAE equations and controls. Only results of the quasi-static time domain simulations are shown since these are the same as those obtained for the dynamic continuation power flow (DCPF) analysis.

Figure 6 shows the QSTDS for the CSIG. In particular Fig. 6 shows the voltage at a representative bus of the distribution

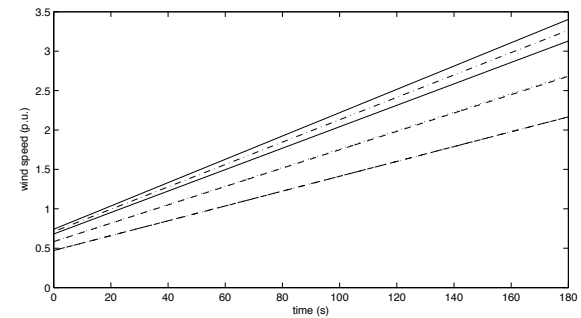


Fig. 5. Wind speed ramps used for the quasi-static time domain simulations.

network. Observe that the system collapses for  $t \approx 18$  s that corresponds to a generation margin of about  $\lambda \approx 1$ , thus well before than the generation margin obtained with the SCPF analysis. This is due to the dynamic model of the induction generator which becomes unstable for a generation level close to 1 p.u.

Figures 7, 8, 10 and 9 show the QSTDS for the DFIG. In particular, Fig. 7 shows the voltage at a representative bus of the distribution network. Interestingly, the system does not collapse thanks to the active power control (see Fig. 8) and pitch control (see Fig. 9) of the DFIGs. These controls are enforced only for super-synchronous speeds. Figure 9 shows the reactive powers generated by the DFIGs. The reactive

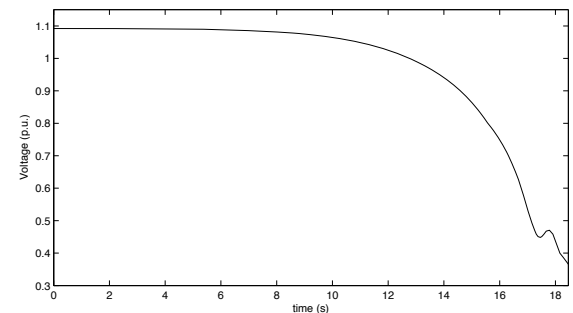


Fig. 6. CSIG and QSTD. Voltage magnitude at bus 29.

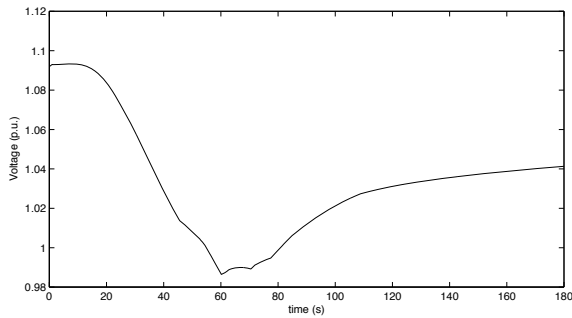


Fig. 7. DFIG and QSTD. Voltage magnitude at bus 29.

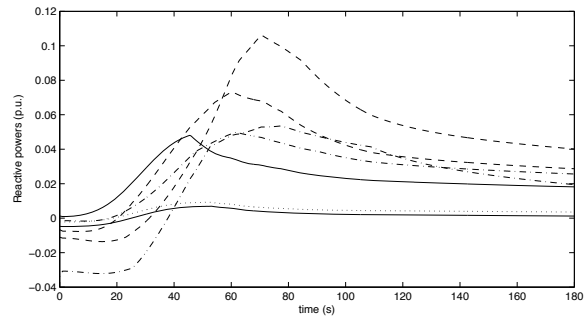


Fig. 10. DFIG and QSTD. Reactive power generated by the EWGs.

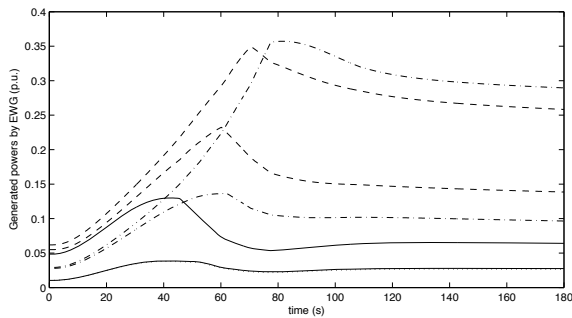


Fig. 8. DFIG and QSTD. Active power generated by the EWGs.

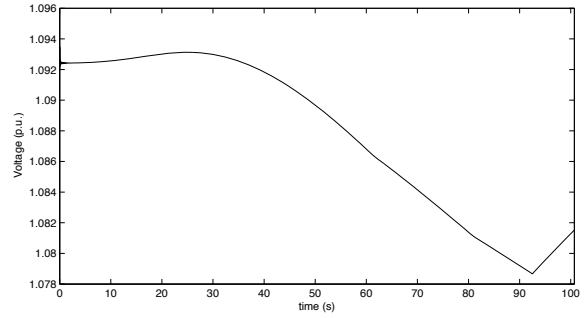


Fig. 11. DDSG and QSTD. Voltage magnitude at bus 29.

powers are limited by the voltage controllers of DFIGs.

Figure 11 shows the QSTDs for the DDSG. In particular Fig. 11 shows the voltage at a representative bus of the distribution network. In this case, the system does collapse, even though for a generation level higher than that obtained with the SCPF analysis. The increase in the generation level is due to the active power and pitch controls of the DDSGs. However, the controllers are not able to avoid the instability of the synchronous generators for high wind power values. Once again, the collapse cannot be anticipated based on voltage measures.

Figure 12 shows the wind speeds used for the time domain simulations (TDS). The wind speeds are composed of a 15 s ramp, a gust component, and a white noise component. The

ramp is realistic but quite fast, in order to force fast dynamics of EWGs.

Figure 13 shows the TDS for the DFIG. In particular Fig. 13 shows the voltage at a representative bus of the distribution network. The TDS gives same results as the QSTDs. This result is general and valid for all EWG models. This fact allows concluding that a detailed wind model is not necessary for voltage stability studies of distribution networks with high wind power penetration.

### V. CONCLUSIONS

This paper presents a variety of simulations for assessing voltage stability of distribution networks with high wind power penetration. Three EWGs models are considered, namely,

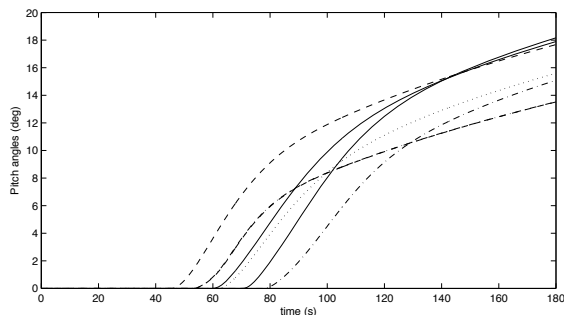


Fig. 9. DFIG and QSTD. Pitch angles  $\theta_p$  of the EWGs.

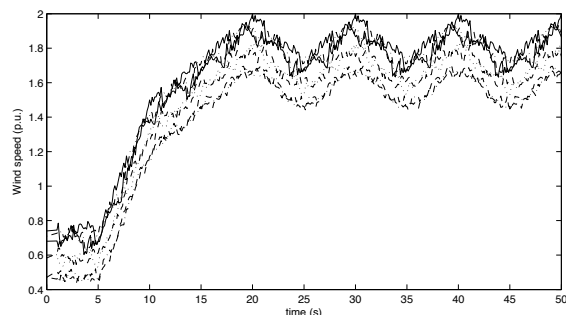


Fig. 12. Wind speed ramps used for the time domain simulations.

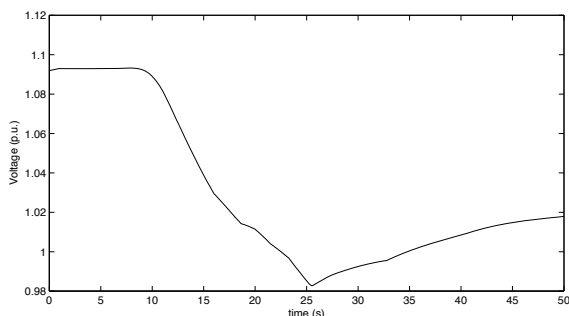


Fig. 13. DFIG and TD. Voltage magnitude at bus 29.

constant-speed induction generator; doubly-fed induction generator; and direct-drive synchronous generator.

Relevant conclusions are as follows:

- 1) The static generation margin of the system can be improved if the EWGs regulate the voltage.
- 2) Accurate dynamic models of EWGs are necessary to assess precise voltage stability limits of the network. Standard static CPF analysis based on constant PQ or PV generator models can lead to misleading conclusions. In particular, for CSIGs, the collapse can occur before than what anticipated with the static analysis.
- 3) EWG controllers are effective in enhancing the generation margin of the distribution system. In the case of DFIGs, controllers eliminate the induction generator instabilities that are shown by CSIG and can even avoid the voltage collapse. In the case of DDSG, controllers cannot avoid instability of the synchronous generators.
- 4) Dynamic continuation power flow, quasi-static time domain simulations and time domain simulations provide almost identical results. Thus it is preferable to use quasi-static time domain simulations because they can be solved with standard power system programs and do not need a detailed model of the wind speed.

Further research is needed on this topic. An interesting issue is to set up a static EWG model able to provide an adequate information about voltage stability limits and voltage collapse.

## REFERENCES

- [1] E. DeMeo, W. Grant, M. R. Milligan, and M. J. Schuenger, "Wind Plant Integration: Costs, Status, and Issues," *IEEE Power & Energy Magazine*, pp. 38–46, November–December 2005.
- [2] P. B. Eriksen, T. Ackerman, H. Abildgaard, P. Smith, W. Winter, and J. Rodríguez-García, "System Operation with High Wind Penetration: The Challenges of Denmark, Germany, Spain, and Ireland," *IEEE Power & Energy Magazine*, pp. 65–74, November–December 2005.
- [3] R. Zavadil, N. Miller, A. Ellis, and E. Muljadi, "Making Connections: Wind Generation Challenges and Progress," *IEEE Power & Energy Magazine*, pp. 26–37, November–December 2005.
- [4] E. Muljadi and C. P. Butterfield, "Pitch-controlled Variable-speed Wind Turbine Generation," *IEEE Transactions on Industry Applications*, vol. 37, no. 1, pp. 240–246, Jan. 2001.
- [5] J. Fan and S. K. Salman, "The Effect of Integration of Wind Farms into Utility Network on Voltage Control due to the Co-ordination of AVC Relays," in *Proceedings of the Fourth International Conference on Advances in Power System Control, Operation and Management, APSOM-97*, vol. 1, Nov. 1997.

- [6] N. D. Hatzigryriou, T. S. Karakatsanis, and M. P. Papadopoulos, "The Effect of Wind Parks on the Operation of Voltage Control Devices," in *Proceedings of the 14th International Conference and Exhibition on Electricity Distribution. Part 1. Contributions*, vol. 5, June 1997.
- [7] A. Miller, E. Muljadi, and D. S. Zinger, "A Variable Speed Wind Turbine Power Control," *IEEE Transactions on Energy Conversion*, vol. 12, no. 2, pp. 181–186, June 1997.
- [8] J. G. Slootweg, "Wind Power: Modelling and Impact on Power System Dynamics," Ph.D. dissertation, Delft University of Technology, Delft, Netherlands, 2003.
- [9] R. Cano-Marín, A. Gómez-Expósito, and M. Burgos-Payán, "Wind Energy Integration in Distribution Networks: A Voltage-Stability Constrained Case Study," in *Proceedings of the VI Bulk Power System Dynamics and Control*, Cortina d'Ampezzo, Italy, Aug. 2004.
- [10] Z. Fengquan, G. Joos, and C. Abbey, "Voltage Stability in Weak Connection Wind Farms," in *Proceedings of the IEEE Power Engineering Society General Meeting*, San Francisco, CA, June 2005.
- [11] W. Freitas, J. C. M. Vieira, L. C. P. da Silva, C. M. Affonso, and A. Morelato, "Long-term Voltage Stability of Distribution Systems With Induction Generators," in *Proceedings of the IEEE Power Engineering Society General Meeting*, San Francisco, CA, June 2005.
- [12] L. T. Ha and T. K. Saha, "Investigation of Power Loss and Voltage Stability Limits for Large Wind Farm Connections to a Subtransmission Network," in *Proceedings of the IEEE Power Engineering Society General Meeting*, Denver, CO, June 2004.
- [13] M. T. Pålsson, T. Toftvaag, K. Uhlen, and J. O. G. Tande, "Large-scale Wind Power Integration and Voltage Stability Limits in Regional Networks," in *Proceedings of the IEEE Power Engineering Society General Meeting*, Chicago, IL, June 2002.
- [14] —, "Control Concepts to Enable Increased Wind Power Penetration," in *Proceedings of the IEEE Power Engineering Society General Meeting*, Toronto, Canada, June 2003.
- [15] F. Milano, A. J. Conejo, and J. L. García-Dornelas, "Reactive Power Adequacy in Distribution Networks with Embedded Distributed Energy Resources," *ASCE Journal of Energy Engineering*, Apr. 2006, accepted for publication.
- [16] S. N. Liew and G. Strbac, "Maximizing Penetration of Wind Generation in Existing Distribution Networks," *IEEE Proceedings on Generation, Transmission and Distribution*, vol. 3, no. 149, pp. 256–262, May 2002.
- [17] C. A. Cañizares, "Voltage Stability Assessment: Concepts, Practices and Tools," IEEE/PES Power System Stability Subcommittee, Final Document, Tech. Rep. SP101PSS, Aug. 2002, available at <http://www.power.uwaterloo.ca>.
- [18] S. Greene and I. Dobson, "Voltage Collapse Margin Sensitivity Methods applied to the Power System of Southwest England," Feb. 1998, available at <http://www.pserc.wisc.edu>.
- [19] F. Milano, "PSAT, Matlab-based Power System Analysis Toolbox," 2007, available at <http://www.uclm.es/area/gsee/Web/Federico>.
- [20] J. G. Slootweg, H. Polinder, and W. L. Kling, "Representing Wind Turbine Electrical Generating Systems in Fundamental Frequency Simulations," *IEEE Transactions on Power Systems*, vol. 20, no. 3, pp. 1199–1206, Aug. 2005.
- [21] V. Akhmatov, H. Knudsen, and A. H. Nielsen, "Advanced Simulation of Windmills in the Electric Power Supply," *International Journal of Electric Power and Energy Systems*, vol. 22, no. 6, pp. 421–434, Aug. 2000.
- [22] F. Milano, "An Open Source Power System Analysis Toolbox," *IEEE Transactions on Power Systems*, vol. 20, no. 3, pp. 1199–1206, Aug. 2005.



**Federico Milano** (M'03) received from the University of Genoa, Italy, the Electrical Engineering degree and the Ph.D. degree in 1999 and 2003, respectively. From 2001 to 2002 he worked at the University of Waterloo, Canada, as a Visiting Scholar. He is currently an associate Professor at the University of Castilla-La Mancha, Ciudad Real, Spain. His research interests include voltage stability, electricity markets and modeling of electric power systems.